Requirements and possible simplifications for multi-ionic transport models ? Case of concrete subjected to wetting-drying cycles in marine environment

Anthony Soive, Véronique Baroghel Bouny, van Quan Tran

REQUIREMENTS AND POSSIBLE SIMPLIFICATIONS FOR MULTIONIC TRANSPORT MODELS – CASE OF CONCRETE SUBJECTED TO WETTING-DRYING CYCLES IN MARINE ENVIRONMENT

Anthony Soive[1,2]

Véronique Baroghel-Bouny[3]

Van-Quan Tran[2]

[1] Centre d'Etudes et d'Expertises sur les Risques, l'Environnement, la Mobilité et l'Aménagement (Cerema), Nantes, France

[2] Institut de Recherche en Génie Civil et Mécanique (GeM), UMR-CNRS 6183, Ecole Centrale de Nantes, France

[3] Materials and Structures Department, FM^{2}D Laboratory, Paris-Est University, IFSTTAR, Champs-sur-Marne, Paris, France

ABSTRACT: In this paper, a physically and chemically based model, which describes coupled ion-moisture transport, is used to simulate chloride ingress in concrete elements subjected to wetting-drying cycles in marine environment. Various assumptions are tested, in order to quantify the influence of taking into account thermochemistry such as Friedel's and Kuzel's salts precipitation on the ingress kinetics or to underline the differences between complex model and very simple one (assuming saturated conditions in the latter case). Numerical simulations are compared to experimental chloride concentration profiles. Experimental data were obtained on an OPC concrete specimens exposed to 6h/6h seawater wetting-drying cycles in lab (where RH and T are controlled).

The results show that when the initial amounts of hydration products are known, the assessment of the chloride binding parameters is not needed. In addition, including thermochemistry in the model improves the predictions, in particular with regard to pH value that can be used as rebar depassivation evaluation criterion. Moreover, the boundary layer thickness that reflects the evaporation kinetics is not an important parameter for the studied concretes. Updating at each time step the transport properties in order to account for dissolution / precipitation of mineral species does not change very much the chloride profiles as well. Furthermore, simulations carried out in saturated conditions do not provide similar results to those obtained when accounting for wetting-drying cycles for the studied concrete. Nevertheless, it may be possible to use a simple model, and thus avoid the problematic assessment of the "intrinsic" permeability, to predict RC service life in the case of low-permeability concretes.

Keywords: chloride ingress, wetting-drying cycles, thermochemical model, concrete

Anthony Soive is a researcher at Cerema, a new public body in support of national and local authorities in the field of sustainable development. His research field covers RC durability.

Véronique Baroghel-Bouny is the Director of the Mix-design, microstructure, modelling and durability (FM^2D) Laboratory at IFSTTAR. She is in charge of various research projects and working groups. Her research field covers microstructure of cement-based materials and various aspects of RC durability with special interest in new concretes.

Van-Quan TRAN is a PhD student at Ecole Centrale de Nantes, France. He works on thermochemical model for simulating corrosion initiation in concrete subjected to seawater.

INTRODUCTION

The main deterioration cause for reinforced concrete structures exposed to marine environment is the corrosion induced by chloride penetration into concrete. Owing to the expensive costs of repair and maintenance it is highly requested to develop reliable models intended to predict the chloride concentration profiles in tidal zone where the corrosion is occurring faster than in the other zones in the structure.

Many studies have been dedicated to the modeling of chloride transport through unsaturated concrete by taking into account diffusion and convection. Some are based on an approach that describes moisture ingress as a pure fickian process [1]–[5]. They used semi-empirical laws found by fitting experimental data to get the relationship between moisture diffusivity and the chloride diffusion coefficient. Others are coupled moisture-multionic transport models that take into account advection and diffusion process for liquid and gas [6], [7]. However, these models have a number of limitations. First, they cannot be applied to all types of concrete since they use empirical relationship for the chloride binding isotherm. Few models take into account both Friedel's salt precipitation and "physical" binding onto C-S-H [8], [9] but they do not have been used with seawater. Second, pH calculation is often missing. However, the aim of chloride transport modelling is to lead to a better understanding of the mechanisms and to a better estimation of the time needed to reach a given critical or threshold value, which induces depassivation, at the first layer of reinforcement. Several threshold expressions need the hydroxyde concentration [10], [11]. Then chloride ion propagation models involve the evolution of the pH in the cementitious material.

Furthermore, transport in unsaturated concrete involves many complex mechanisms. The number of parameter that describes the various phenomena involved can be significant. The modelling requires taking into account the transport of liquid water and that of the gas phase (air and water vapour), and the transport of the ions contained in seawater. With regard to moisture transport, a number of studies have been performed on the drying process and how to model it [12]–[15]. They show that, in addition to water vapour sorption isotherm and to the conventional parameters related to transport ("intrinsic" permeability, and diffusion coefficient), it is necessary to estimate an evaporation layer thickness over which diffusion occurs [16].

Faced with this situation, the main objectives of the study described in the paper is to evaluate the influence of several parameters dedicated to in order to identify possible simplifications and requirements for transport models in concrete subjected to wetting-drying cycles in marine environment. A numerical simulation program for chemically reactive non-isothermal flows of multiphase fluids in porous and fractured media [17], has been used. The interaction between chlorides and monosulphate are deduced from the modelling of the precipitation of salts, such as Friedel's or Kuzel's salts [18], [19]. With regard to the chloride binding onto the C-S-H surface [20], a linear adsorption that depends on the initial C-S-H amount is adopted here by sake of simplicity. The influence of a number of parameters is then evaluated, as the "intrinsic" permeability, the evaporation layer thickness, updating porosity and permeability. The numerical results have been compared to experimental data measured concrete samples subjected to wetting-drying cycles in lab. The differences between a complex model and a very simple one (assuming saturated conditions in the latter case) are also evaluated.

In the present paper, section 1 describes the experimental set-up used for exposing concrete specimens to wetting-drying cycles with natural seawater and controlled environmental conditions. Section 2 depicts the governing equations used to simulate moisture and ionic transport in non-saturated cimentitious materials. Section 3 introduces the predicted and experimental chloride concentration profiles.

EXPERIMENTAL STUDY

Concrete mixtures

The experimental study was carried out on one normal-strength OPC concretes submitted to wetting/drying cycles with seawater in lab (BO). The mix proportions of this concrete are summarized in Table 1. The aggregates are composed of limestone gravel and calcareous and silico-calcareous sand. The cement used is a CEM I 52.5 PM ES CP2. The mix-design principles of these concretes are explained in [21].

Table 1: BO mix-design [21]

Concrete	Limestone gravel 4/20 [$kg.m^{-3}$]	Calcareous and silico-calcareous sand 0/5 [$kg.m^{-3}$]	Cement CEMI 52,5 [$kg.m^{-3}$]	Water [$kg.m^{-3}$]	w/c
BO	1192	744	353	152	0.43

Experimental procedure

The BO concrete was cast in cylindrical specimens (thickness = 100 ± 1mm; diameter = 110mm). After demould, the non-curved surfaces were polished to have plane and clean surfaces. The specimens were immersed into water during 1.5 year. Then, a dense epoxy coating was applied to lateral surface and one face, leaving an exposed plane surface to ensure a one-dimensional flow inside the cylinders.

The samples were submitted to 72-h vacuum saturation with a 0.1N NaOH solution prior to exposure to wetting and drying cycles. Each specimen was exposed to 2 daily cycles of 6 hours of seawater penetration (seawater extracted from the bay of Saint-Brieuc in northern France) and drying for 6 hours. During drying, a fan ensured a well-mixed atmosphere in the chamber. BO samples were exposed during 90 and 180 days. Temperature (T = 20±1°C) and relative humidity (RH = 65±5%) were controlled thanks to an air-conditioning system.

Measurements

Total and free chloride concentration profiles have been measured on cores at given depths. A Profile Grinder was used to extract powder (< 80μm) from the samples over a 50mm disk and allows a 2mm penetration increment. The total chloride concentration (resp. free chloride concentration) has been assessed by means of nitric acid (resp. water) extraction and potentiometric titration (by using a $0.01N AgNO_3$ solution), according to the AFPC-AFREM procedure [22].

MODELLING APPROACH

A physically and chemically based model, which describes coupled ion-moisture transport, is used to simulate chloride ingress in concrete elements subjected to wetting-drying cycles in marine environment. The transport equations for moisture are first exposed. Ionic transport and dissolution / precipitation of mineral species follow.

Moisture transport

The mass balance equation used can be written in a general form (see equation 1 [23]).

$$\frac{d}{dt}\int m^i \, dV = \int J^i . n dS + \int q^i \, dV \quad (1)$$

Which leads to 2 by applying Gauss divergence theorem:

$$\frac{d}{dt} m^i = -div(J^i) + q^i \quad (2)$$

Where m represents mass per volume, J mass flux, q sinks and sources and i labelling the components (water, air). The mass accumulation term and mass fluxes read:

$$m^i = \phi \sum_\beta S_\beta \rho_\beta X_\beta^i \quad (3)$$

$$J^i = \sum_\beta X_\beta^i \left[-k \frac{k_{r_\beta} \rho_\beta}{\mu_\beta} \left(\nabla P_\beta - \rho_\beta g \right) \right] - \sum_\beta \rho_\beta D_\beta^i \nabla X_\beta^i \quad (4)$$

Where $\phi, S_\beta, \rho_\beta, k, k_{r_\beta}, \mu_\beta, P_\beta$ are the porosity accessible to water, degree of saturation, density, "intrinsic" permeability, relative permeability of phase β, dynamic viscosity and pressure of phase β, respectively. X_β^i is the mass fraction of component i present in phase β and D_β^i the diffusion tensor.

The relative permeabilities to liquid and gas is assumed to be expressed as a function of liquid saturation, as proposed by Van Genuchten (see equation 5) [24]., and Corey (see equation 6) [25], respectively.

$$k_{r_l} = \sqrt{\tilde{S}} \left[1 - \left(1 - \tilde{S}^{1/\lambda} \right)^\lambda \right]^2 \quad (5)$$

with $\tilde{S} = \left(S_l - S_{l_r} \right) / \left(S_{l_s} - S_{l_r} \right)$

$$k_{rg} = (1 - S^*)^2 \left(1 - S^{*2} \right) \quad (6)$$

with $S^* = (S_l - S_{lr}) / \left(1 - S_{lr} - S_{rg} \right)$

where Slr and Sgr are residual liquid and gas saturation, respectively.

The liquid pressure is a function of the capillary pressure, Pc, and the gas pressure (see

equation 7). The capillary pressure is assumed to be expressed as a function of liquid saturation, as proposed by Van Genuchten (see equation 8) [24]:

$$P_l = P_g - P_c \quad (7)$$

$$P_c = -P_0 \left(\left[\tilde{S} \right]^{-1/\lambda} \right)^{1-\lambda} \quad (8)$$

In this system of equations, the gaseous phase is assumed to be the result of the mix between two ideal gases (dry air and water vapour). The mix is also considered as ideal leading to the fact that the total gas pressure is equal to the sum of the pressures of the two gases described before. The vapour adsorption and desorption are described by the same parameters that result from equation 10 and the Kelvin equation that express capillary pressure as a function of relative humidity. Skeleton is incompressible and non-expansive.

In addition, several hypotheses were done in order to simplify the system of equations. First, gravity forces are negligible compared to forces due to pressure. Second, relative humidity and liquid pressure are supposed to be independent of the concentration of ions in the solution. This point will be discussed further in the results section. Finally, dynamic viscosity and density are supposed to be independent of the NaCl amount [26].

Ionic transport

In unsaturated porous media, the species transport in the material is driven by convection and diffusion. At a local scale two fluxes are then associated: a diffusive and an advective flux. Fick's first law can approximate the first one where each species has the same diffusion coefficient. This assumption insures the electroneutrality of the system. Fick's first law is preferred here to Nernst-Planck approach since it is simplier and its less computing-time consuming. In addition, in Nernst-Planck approach only primary species (e.g. Na+, Cl-, SO42-…) are supposed to propagate. However, primary species react in the solution to form aqueous complexes (that reactive geochemical transport modelling are able to simulate). Such reactions lead to electronic charges that can be very different from primary species generally used. The advective flux depends on fluid velocity that is calculated by moisture transport model. The total flux is given by the sum of the two fluxes (see equation 9):

$$\boldsymbol{J} = -D_e \nabla \mathbf{C} + u_l C \quad (9)$$

where $\boldsymbol{J}$ is the total flux (kg.m^{-2}.s^{-1}), $\boldsymbol{\nabla}$ is the gradient operator, D_e a tensor of second order which represents the effective ionic diffusion coefficient in the porous media (m^2.s^{-1}), C the concentration of ions in the solution (kg.m^{-3} of solution) and u_l the water velocity vector.

In addition, chloride ions can be bound to the concrete matrix. Nevertheless, in order to avoid the use of empirical parameters for binding isotherm, a thermochemical model is used. Such a model allows one to simulate the precipitation of mineral species (e.g. Friedel's salt). This is described in the next section. For the chloride binding on C-S-H, the model should describe the Stern double layer [27]. However, by sake of simplicity, a linear adsorption is supposed and calculated from the initial C-S-H amount.
Finally, although several ionic species present in the seawater are taken into account in the model, one unique and constant effective diffusion coefficient was adopted. It is considered as a function of tortuosity, τ, porosity, and pure diffusion coefficient of species, D_0 in water:

$$D_e = \Phi \tau S_l D_0 \quad (10)$$

The ionic species in the liquid phase are not supposed to diffuse in the gas phase.

Dissolution / precipitation of mineral species

When the solution is not equilibrium state, one can calculate the ion activity product Q for one mineral species that is the product of the species concentration formed divided by the product of the species concentration consumed. This equilibrium is controled by the law of mass action. The ratio between Q and the thermodynamic solubility product K, enters the definition of the saturation index IS, expressed as:

$$IS = log_{10}\left(\frac{Q}{K}\right) \quad (11)$$

When $IS = 0$, equilibrium is reached. When $IS < 0$, the solution is undersaturated and the mineral species should dissolve. On the contrary, when $IS > 0$ the solution is supersaturated and the mineral species shlould precipitate. Hence, at each time step, Q is calculated for each mineral species and compared to its solubility product.

The geochemical reactions rate is supposed to be large with respect to the ionic and fluid transport processes. In this particular case, the local chemical equilibrium was assumed to be preserved throughout the porous system. This hypothesis is usually valid in most practical cases involving the diffusion of ions in fluid saturated systems [28], [29].

NUMERICAL METHODS AND INPUT DATA

Boundary conditions

During drying, strong capillary forces are present as a result of the gradient between the vapour partial pressures in the material and in the atmosphere. Schlünder [12] and other [13]–[15] works have shown that evaporative fluxes from wet porous surfaces are constrained by the saturation degree of the material and transport properties of the porous medium, and by the vapor transport across the boundary air layer adjacent to the surface [12]–[15]. Under typical natural conditions (airflow velocity U1< 4 m/s), Haghighi et al. showed that the contribution of advection is relatively minor compared to diffusion porous media (pore sizes < 1000 mm) [15]. Nevertheless, in such an approach, it is necessary to estimate an evaporation layer thickness over which diffusion takes place. Gezzehei et al. suggested values between 5 and 20mm by inverse analysis [30].

From a numerical point of view, the most mechanistic approach to simulate evaporation is to define an air-mass fraction in the atmosphere that corresponds to the relative humidity value, and then actually simulate vapor diffusion from the material surface through the laminar boundary layer (the thickness of which depends on surface roughness and wind velocity etc.) to the well-mixed atmosphere [30], [31]. However, by sake of simplicity and recognizing that both relative humidity and capillary pressure reflect a "water potential", evaporation is approximated by imposing a capillary suction in the boundary element. This capillary suction corresponds to the relative humidity in the atmosphere thanks to Kelvin's equation. Then the boundary layer thickness may be an important factor for evaporation kinetics. Unfortunately,

this thickness is very difficult to assess. Gezzehei et al. suggested values between 5 and 20mm [30] by inverse analysis. These extreme values will be tested in this study.

During wetting, 100% HR is imposed and the concrete is in contact with seawater. The ionic species concentration present in the Atlantic ocean seawater and adopted here are given in table 4. By sake of simplicity and due to convergence difficulties of the wetting-drying model, dissolved CO_2 is not considered in the seawater composition.

Table 2: seawater ionic composition for Atlantic ocean [mol.l^{-1}]

Cl^-	Ca^{2+}	SO_4^{2-}	K^+	Mg^{2+}	Na^+
0.546	$9.97\ 10^{-3}$	$2.76\ 10^{-2}$	$9.71\ 10^{-3}$	$5.22\ 10^{-2}$	0.459

Hydrated concrete properties and mineral species

The use of a coupled transport/thermochemical model, in order to model the propagation of ions in concrete permits to avoid the use of empirical parameters such as binding isotherm parameters that are dependent of the concrete mix-design. Nevertheless, the initial amount of the various hydration products in the concrete is required as input data. A model of hydratation is used, based on Thiery et al. work [32] in order to assess such data (see Table 3).

Table 3: BO phase results with hydration model

Phase	Formulation	volume fraction of solid
C_3AH_6	$Ca_3Al_2(OH)_{12}$	$5.88\ 10^{-3}$
$Jennite$	$Ca_{1.67}SiO_2(OH)_{3.33}{:}H_2O$	$1.31\ 10^{-1}$
$Ettringite$	$Ca_6Al_2(SO_4)_3(OH)_{12}{:}26H_2O$	$2.23\ 10^{-18}$
$Monosulphate$	$Ca_4Al_2(SO_4)(OH)_{12}{:}6H_2O$	$1.63\ 10^{-2}$
$Portlandite$	$Ca(OH)_2$	$4.34\ 10^{-2}$

A database has been built according to [33]. The C-S-H (assumed here as Jennite) was considered as a single phase gel. Table 4 shows a part of the database where the mineral phases were supposed to react.

Table 4: thermodynamic properties at T=25°C for the hydrated products and mineral species that may precipitate

Mineral	$\log(K)$
$C_3AH_6 + 12H^+ \rightarrow 3Ca^{2+} + 2Al^{3+} + 12H_2O$	80.88
$Jennite + 18H^+ \rightarrow 9Ca^{2+} + H_4SiO_4(aq) + 8H_2O$	147.34
$Ettringite + 12H^+ \rightarrow 2Al^{3+} + 6Ca^{2+} + 3SO_4^{2-} + 38H_2O$	56.67
$Monosulphate + 12H^+ \rightarrow 4\,Ca^{2+} + 2Al^{3+} + {SO_4}^{2-} + 18H_2O$	72.44
$Portlandite + 2H^+ \rightarrow Ca^{2+} + 2H_2O$	22.76
$Halite \rightarrow Na^+ + Cl^-$	1.60
$Friedel\_Salt + 12.05H^+ \rightarrow 2Al^{3+} + 4Ca^{2+} + 1.95Cl^- + 16.05H_2O$	76.14
$Kuzel\_Salt + 12H^+ \rightarrow 2Al^{3+} + 4Ca^{2+} + 1Cl^- + 0.5{SO_4}^{2-} + 18H_2O$	73.24

Numerical procedure

The simulations were performed in 1D, due to the symmetry of the system. A simple mesh composed of one 100-element row was used and represented the length of the sample. Calculations are managed with a code developed in Python [34]. This allows one to apply wetting-drying cycles by 1-hour time step without effort. At each time step a restart is running with the previous time step results.

NUMERICAL RESULTS AND COMPARISON WITH EXPERIMENTAL DATA

Friedel's and Kuzel's salts

A simulation has been carried out on BO concrete with the proposed model. Figure 1 shows the precipitation and dissolution of concrete mineral species as a function of depth after 90 wetting-drying cycle days. It indicates that Friedel's salt and halite (NaCl) do not precipitate. Only Kuzel's salt is able to precipitate by consuming monosulphate and C_3AH_6. This can be explained by the presence of sulphate in seawater. The model also predicts precipitation of ettringite in the first millimetres. The pH remains basic (between 12 and 14, see Figure 1) due to the presence of portlandite, except in the first millimetres due to leaching of the concrete and the total dissolution of portlandite. This leaching also leads to the important decrease of the Kuzel's salt amount (see also Figure 2 b).

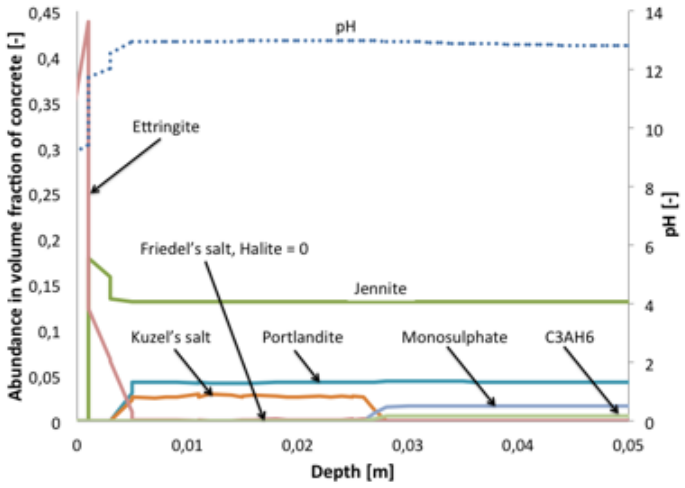

Figure 1: Precipitation and dissolution of concrete mineral species as a function of depth after 90 wetting-drying cycles days

Influence of the "intrinsic" permeability value

The influence of the "intrinsic" permeability value is evaluated by calculating free and total chloride concentrations as a function of depth with several permeability values (cf. Figure 2 and Figure 4). Three permeability values are tested here: 3.10^{-21}, 8.10^{-21} and 3.10^{-20} m^2. The

first two were assessed by indirect method and Katz-Thomson formula [37], while the third one is 10 times the first one in order to test a concrete that may be micro-cracked.

Figure 2 a) shows that a permeability value of 8.10^{-21} provides the free chloride concentration profile very close to the experimented one. Moreover, smaller the permeability value faster the free chloride diffusion. This can be explained by drawing the "drying depth" as a function of the permeability values after 180 days of exposure and time (Figure 3 a and b, respectively). This depth can be defined as the depth over which drying and wetting profiles are the same. Figure 3 b) shows that the saturation profiles after only 2 days are very close to profiles after 180 days. Furthermore, the saturation profiles for various permeability values (Figure 3 a) show that the greater the permeability value the greater the drying depth. This result was expected since the liquid water transport is easier for more permeable material. The drying depth values are 20mm, 40mm et 90mm for permeability values of 3.10^{-21}, 8.10^{-21} and 3.10^{-20} m^2, respectively.

Total chloride concentration profiles are not satisfying since they are not close to experimental data (see Figure 4). The main explanation is that the amount of ettringite is overestimated (see Figure 1) since the sulphate is not adsorbed onto C-S-H in the model. Hence, Kuzel's salt dissolves in the first millimetres. Other explanations can be given. First, adopting a linear "physical" adsorption isotherm in order to approximate adsorption isotherm onto the C-S-H leads to an underestimation of the bound chlorides for low free chloride concentration and to an overestimation for the high concentration compared to Freundlich or Langmuir isotherms. Second, the leaching in the first millimetres is probably overestimated since the model does not account for the presence of dissolved CO_2 in seawater. Hence the possible precipitation of monocarbonate that is more stable than monosulphate should limit the dissolution monosulphate amount. Third, kinetics of precipitation are not taken account in this study, in particular for Kuzel's salt. However, the required thermodynamical data are missing in the literature to the author's knowledge.

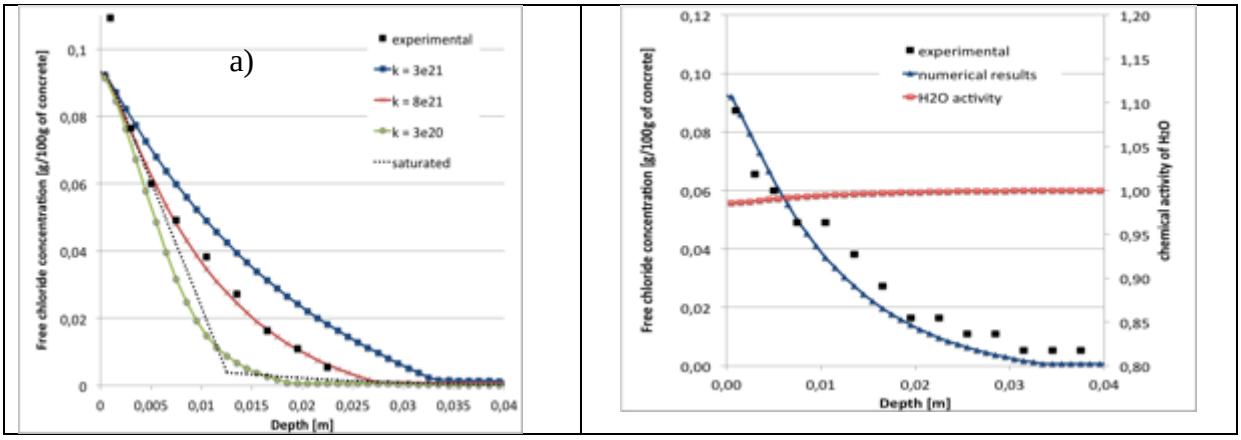

Figure 2: Free chloride concentration as a function of the depth, for BO a) in various cases (several permeability values and case of saturated concrete) after 90 days of exposure and b) 180 days for $k=8e^{-21}m^2$

The previous results are confirmed for concrete exposed to wetting-drying cycles during 180 days (**Erreur ! Source du renvoi introuvable.**).

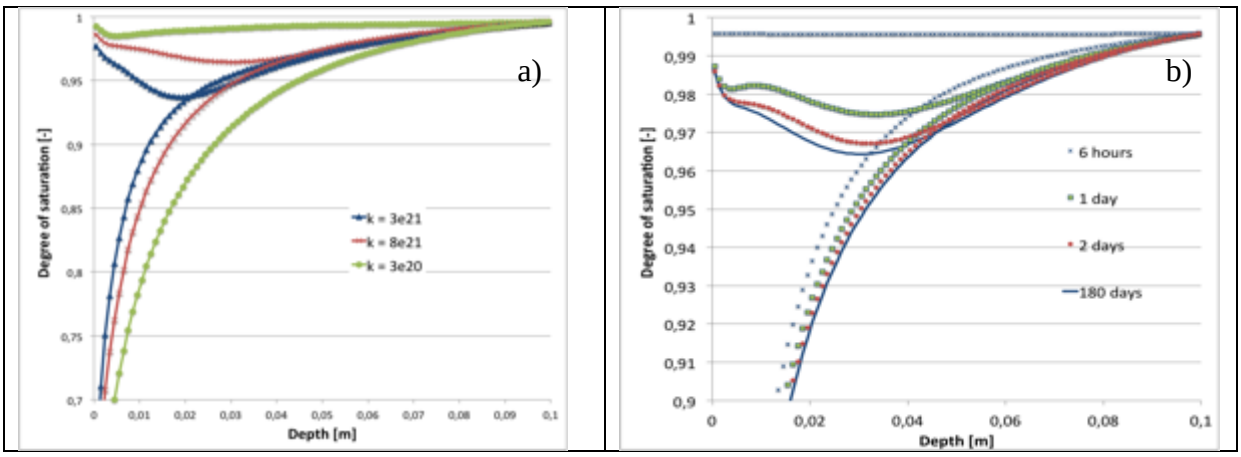

Figure 3: a) Evolution of saturation degree vs depth for a) several "intrinsic" permeability values and b) time evolution (intrinsic permeability = 8 10^{-21})

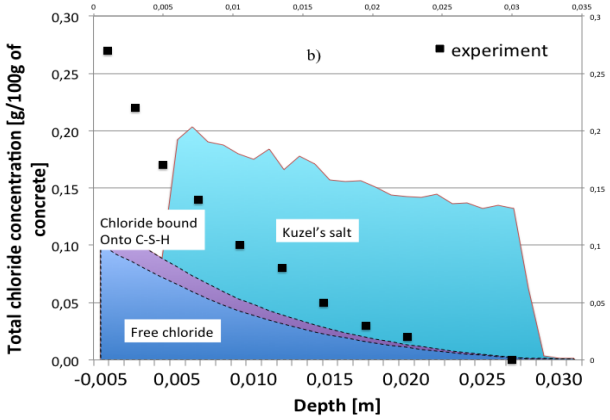

Figure 4: Total chloride concentration as a function of the depth for BO after 90 days of exposure

It should be noted that the vapor-pressure lowering caused by dissolved salts is not taken into account. The pore solution is considered as a dilute solution. This hypothesis is confirmed by the calculation of the chemical activity of water which remains very close to 1 (see Figure 2 b).

Influence of the boundary layer thickness

The values of the boundary layer thickness calculated by Ghezzehei et al. [30] have been tested. They correspond to different environmental conditions in which specimens are exposed: wind are present (d=5 mm) or not (d=20 mm). Despite the presence of a fan in the chamber the specimens are not exposed to ventilation, since the surface in contact with seawater is the bottom of the specimens. A value of 20 mm should rather be chosen.

The results show that free and total chloride concentration profiles are not very sensitive to the thickness of the boundary layer (see

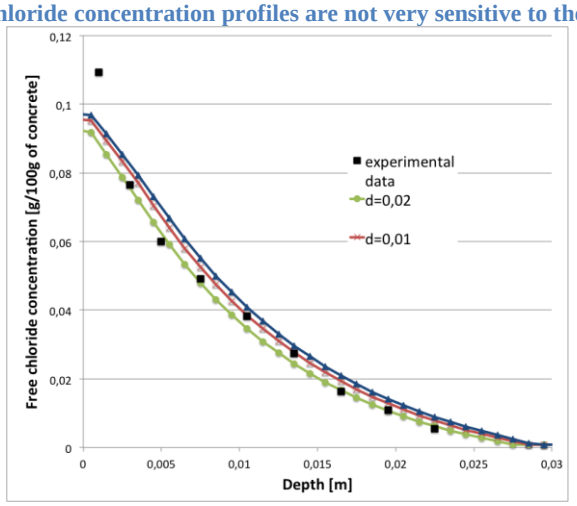

Figure 5). This can be explained by the fact that the wetting-drying cycles frequency is relatively high and that the drying depth is small as explained in the previous section (see Figure 3).

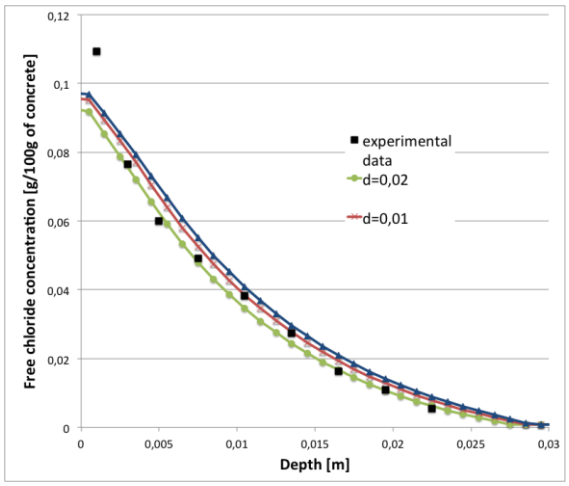

Figure 5: a) Free chloride concentration and b) total chloride concentration as a function of the depth for BO after 90 days of exposition and for various boundary layer thickness values (intrinsic permeability = 8 10^{-21})

Wetting-drying cycles vs. saturated

Considering the high frequency of the wetting-drying cycles, it can be relevant to compare the results provided by the model described here to those obtained by means of a simpler model assuming saturated conditions. Such a model is less time consuming and the number of parameters is smaller. Figure 2 shows that the free chloride profile is not very close to experimental results. On the other hand, the total chloride concentration profile seems better compared to the results obtained with the more complex model. Nevertheless, it is not reasonable, in the case considered, to assume that the concrete is permanently saturated. For such an assumption the concrete intrinsic permeability value should be higher than the value suggested by Figure 3.

Effect of discounting transport properties

Transport properties can be updated by calculating the material porosity ϕ as a function of the volumes of dissolved and precipitated mineral species (see equation 12). Hence, the permeability can be expressed thanks to Carman-Kozeny [38] empirical law (see equation 13).

$$\phi = 1 - \sum_{i=1}^{n} f_{r_i} \quad (12)$$

where n is the number of minerals, f_{r_i} is the volume fraction of mineral m in the material (Vmineral/Vmedium, including porosity).

$$k = k_i \frac{(1-\phi_i)^2}{(1-\phi)^2} \left(\frac{\phi}{\phi_i}\right)^3 \quad (13)$$

The results show that the effect of the permeability updating is limited. The effect on the edge of the specimen in contact with seawater seems to be better modelled. Nevertheless, such an updating needs to be used with caution. First, the change of average porosity is an approximation of the poral distribution one. Second, the actual relationship between porosity and permeability is still an open debate.

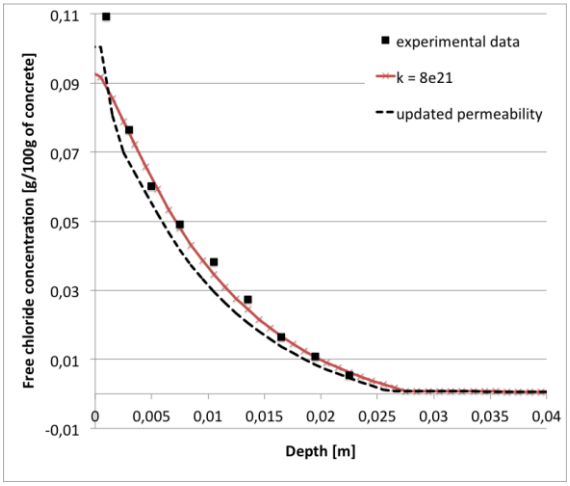

Figure 6: a) Free chlorides concentration as a function of depth for BO after 90 days of exposure. Comparison between profiles with and without properties actualization

CONCLUSION

The main objective of the study was to evaluate the influence of several parameters in order to identify possible simplifications and requirements for transport models in concrete subjected to wetting-drying cycles in marine environment. A physically and chemically based model, which describes coupled ion-moisture transport, was used to simulate chloride ingress in concrete elements subjected to wetting-drying cycles in marine environment. The influence of a number of parameters is then evaluated, such as the “intrinsic” permeability, the boundary layer thickness, updating porosity and permeability. Numerical simulations were compared to experimental chloride concentration profiles obtained on an OPC concrete

specimen exposed to 6h/6h seawater wetting-drying cycles in lab (where RH and T are controlled).

The results show that the “intrinsic” permeability value plays a significant role on the chloride propagation kinetics and the drying depth value. On the other hand, the boundary layer thickness that reflects the evaporation kinetics is not an important parameter for the studied concrete. Updating at each time step the transport properties in order to account for dissolution / precipitation of mineral species does not change very much the chloride profiles as well. Furthermore, simulations carried out in saturated conditions do not provide very good results compared to those obtained when accounting for wetting-drying cycles for the studied concrete. Nevertheless, it may be possible to use a simple model, and thus avoid the problematic assessment of the “intrinsic” permeability, to predict RC service life in the case of low-permeability concretes. Finally, including reactive geochemical modelling in the model improves the predictions, in particular with regard to pH value that can be used as rebar depassivation evaluation criterion.

However, the model needs further improvements such as a complete description of the adsorbed ionic species onto mineral species such as C-S-H. Furthermore, the effect of CO_2 has to be considered since it reacts with monosulphate to precipitate monocarbonate that is more stable than monosulphate in the presence of chloride.

REFERENCES

[1] A. V. Saetta, R. Scotta, and R. Vitaliani, “Analysis of chloride diffusion into partially saturated concrete,” *ACI Mater. J.*, vol. 90, no. 5, pp. 441–451, 1993.

[2] A. Ababneh, F. Benboudjema, and Y. Xi, “Chloride penetration in non saturated concrete,” *J. Mater. Civ. Eng.*, vol. 15, no. 2, pp. 183–191, 2003.

[3] E. Samson, J. Marchand, K. a. Snyder, and J. J. Beaudoin, “Modeling ion and fluid transport in unsaturated cement systems in isothermal conditions,” *Cem. Concr. Res.*, vol. 35, no. 1, pp. 141–153, Jan. 2005.

[4] S. J. H. Meijers, J. Bijen, R. Borst, and A. Fraiij, “Computational results of a model for chloride ingress in concrete including convection, drying- wetting cycles and carbonation,” *Mater. Struct.*, vol. 38, no. 2, pp. 145–154, 2005.

[5] P. O. Iqbal and T. Ishida, “Modeling of chloride transport coupled with enhanced moisture conductivity in concrete exposed to marine environment,” *Cem. Concr. Res.*, vol. 39, no. 4, pp. 329–339, Apr. 2009.

[6] V. Baroghel-Bouny, M. Thiéry, and X. Wang, “Modelling of isothermal coupled moisture–ion transport in cementitious materials,” *Cem. Concr. Res.*, vol. 41, no. 8, pp. 828–841, Aug. 2011.

[7] B. Mickae and X. Wang, “Performance-based assessment of durability and prediction of RC structure service life : transport properties as input data for physical models,” pp. 1669–1691, 2014.

[8] E. Samson and J. Marchand, “Modeling the effect of temperature on ionic transport in cementitious materials,” *Cem. Concr. Res.*, vol. 37, pp. 455–468, 2007.

[9] T. Q. Nguyen, “Modélisations physico-chimiques de la pénétration des ions chlorures dans les matériaux cimentaires.,” Ecole Nationale des Ponts et Chaussées, 2007.

[10] D. A. Hausmann, “Steel corrosion in concrete. How does it occur?,” *Mater. Prot.*, vol. 6, pp. 19–23, 1967.

[11] V. K. Gouda, “Corrosion and corrosion inhibition of reinforcing steel. I. Immersed in alkaline solutions,” *Br. Corros. J.*, vol. 5, pp. 198–203, 1970.

[12] E.-U. Schlünder, “On the mechanism of the constant drying rate period and its relevance to diffusion controlled catalytic gas phase reactions,” *Chem. Eng. Sci.*, vol. 43, no. 10, pp. 2685–2688, 1988.

[13] P. Lehmann, S. Assouline, and D. Or, “Characteristic lengths affecting evaporative drying of porous media,” *Phys. Rev. E*, vol. 77, 2008.

[14] E. Shahraeeni, P. Lehmann, and D. Or, “Coupling of evaporative fluxes from drying porous surfaces with air boundary layer : Characteristics of evaporation from discrete pores,” *Water Resour. Res.*, vol. 48, pp. 1–15, 2012.

[15] E. Haghighi, E. Shahraeeni, P. Lehmann, and D. Or, “Evaporation rates across a convective air boundary layer are dominated by diffusion,” *Water Resour. Res.*, vol. 49, pp. 1602–1610, 2013.

[16] W. M. Rohsenow and H. Choi, *Heat, mass and momentum transfer*, Prentice H. 1961.

[17] T. Xu, N. Spycher, and E. Sonnenthal, “TOUGHREACT User’s Guide: A Simulation Program for Non-isothermal Multiphase Reactive Transport in Variably Saturated Geologic Media, version 2.0,” *Lawrence Berkeley …*, no. October. 2012.

[18] H. Kuzel, “Röntgenuntersuchung im system 3CaO.Al2O3.CaSO4.nH2O-3CaO.Al2O3.CaCl2.nH2O-H2O,” *Neues Jahrb. für Mineral. Monatschefte*, vol. 13, pp. 193–200, 1966.

[19] F. P. Glasser, A. Kindness, and S. A. Stronach, “Stability and solubility relationships in AFm phases Part I. Chloride, sulfate and hydroxide,” *Cem. Concr. Res.*, vol. 29, pp. 861–866, 1999.

[20] J. J. Beaudoin, V. S. Ramachandran, and R. F. Feldman, “Interaction of chloride and C-S-H,” *Cem. Concr. Res.*, vol. 20, pp. 875–883, 1990.

[21] V. Baroghel-Bouny, M. Dierkens, X. Wang, A. Soive, M. Saillio, M. Thiéry, and B. Thauvin, “Ageing and durability of concrete in lab and in field conditions: investigation of chloride penetration,” *J. Sustain. Cem. Mater.*, vol. 2, no. 2, pp. 67–110, Jun. 2013.

[22] T. Chaussadent and G. Arliguie, “AFREM test procedures concerning chlorides in concrete: extraction and titration methods,” *Mater. Struct.*, vol. 32, no. 217, pp. 230–234, 1999.

[23] T. Xu, E. Sonnenthal, N. Spycher, L. Zheng, N. Miller, and K. Pruess, “TOUGHREACT V3.0-OMP Reference Manual: A Parallel Simulation Program for Non-Isothermal Multiphase Geochemical Reactive Transport.” Lawrence Berkeley National Laboratory, Berkeley, 2014.

[24] M. T. Van Genuchten, “A Closed-form Equation for Predicting the Hydraulic Conductivity of Unsaturated Soils 1,” *Soil Sci. Soc. Am. J.*, vol. 44, pp. 892–898, 1980.

[25] A. T. Corey, “The Interrelation Between Gas and Oil Relative Permeabilities,” *Prod. Mon.*, pp. 38–41, 1954.

[26] D. Archer and R. Carter, “Thermodynamic properties of the NaCl + H2O system,” *J. Phys. Chem.*, vol. 104, pp. 8563–8584, 2000.

[27] D. A. Dzombak and F. M. M. Morel, *Surface complexation modeling*, Wiley Inte. New York, 1990.

[28] E. Samson and J. Marchand, “Modeling the transport of ions in unsaturated cement-based materials,” *Comput. Struct.*, vol. 85, pp. 1740–1756, 2007.

[29] R. Barbarulo, J. Marchand, K. A. Snyder, and S. Prene, “Dimensional analysis of ionic transport problems in hydrated cement systems Part 1. Theoretical considerations,” *Cem. Concr. Res.*, vol. 30, pp. 1955–1960, 2000.

[30] T. A. Ghezzehei, R. C. Trautz, S. Finsterle, P. J. Cook, and C. F. Ahlers, “Modeling Coupled Evaporation and Seepage in Ventilated Cavities,” pp. 806–818, Jul. 2004.

[31] S. Finsterle and K. Pruess, “Solving the estimation-identification problem in two-phase flow modeling,” *Water Resour. Res.*, vol. 31, no. 4, pp. 913–924, 1995.

[32] M. Thiery, G. Platret, E. Massieu, G. Villain, and V. Baroghel-Bouny, “Un modèle d’hydratation pour le calcul de la teneur en portlandite des matériaux cimentaires comme donnée d’entrée des modèles de carbonatation,” in *Journées Ouvrages d’Art du réseau des L.P.C.*, 2005.

[33] P. Blanc, A. Lassin, and P. Piantone, “Thermoddem: a database devoted to waste minerals,” Orléans, France, 2007.

[34] G. van Rossum, “Python tutorial,” Amsterdam, 1995.

[35] A. Croucher, “Pytough: a python scripting library for automating tough2 simulations,” in *New Zealand Geothermal Workshop 2011*, 2011.

[36] K. Pruess, C. Oldenburg, and G. Moridis, “Tough2 user’s guide, version 2.” 2012.

[37] V. Baroghel-Bouny, “Water vapour sorption experiments on hardened cementitious materials. Part II: Essential tool for assessment of transport properties and for durability prediction,” *Cem. Concr. Res.*, vol. 37, no. 3, pp. 438–454, Mar. 2007.

[38] J. Bear, *Dynamics of fluids in porous media*. New York: Dover Publication, 1972.